

QUANTIFYING THE PERFORMANCE OF FORCE-FREE EXTRAPOLATION METHODS USING KNOWN SOLUTIONS

G. BARNES¹

High Altitude Observatory, National Center for Atmospheric Research, P.O. Box 3000, Boulder, CO 80307; barnesg@hao.ucar.edu

K. D. LEKA

Colorado Research Associates Division, NorthWest Research Associates, Inc., 3380 Mitchell Lane, Boulder, CO 80301;
leka@cora.nwra.com

AND

M. S. WHEATLAND

School of Physics, University of Sydney, NSW 2006, Australia; m.wheatland@physics.usyd.edu.au

Received 2005 October 13; accepted 2005 December 15

ABSTRACT

We outline a method for quantifying the performance of extrapolation methods for magnetic fields. We extrapolate the field for two model cases, using a linear force-free approach and a nonlinear approach. Each case contains a different topological feature of the field that may be of interest in solar energetic events. We are able to determine quantitatively whether either method is capable of reproducing the topology of the field. In one of our examples, a subjective evaluation of the performance of the extrapolation suggests that it has performed quite well, while our quantitative score shows that this is not the case, indicating the importance of being able to quantify the performance. Our method may be useful in determining which extrapolation techniques are best able to reproduce a force-free field and which topological features can be recovered.

Subject headings: magnetic fields — methods: numerical — Sun: corona

1. INTRODUCTION

The atmosphere of the Sun is the source of a wide range of energetic events, radiation, and particle acceleration, including coronal mass ejections, flares, and the solar wind. All of these, in some way, involve the magnetic field in the solar corona, and many of them are believed to be associated with magnetic reconnection. Thus, it is important to determine the coronal magnetic field and particularly to understand the topology of the field as it relates to reconnection.

Although some measurements of the magnetic field in the corona do exist (e.g., Brosius et al. 2002; Lin et al. 2004), it is more common for the magnetic field to be measured at the photosphere, from which the coronal magnetic field is extrapolated. The first extrapolations were based on potential field models, in which there are no electric currents present in the corona. However, since vertical currents are measured at the photosphere, it is clear that the coronal magnetic field is not potential.

A natural extension to potential field models are force-free models, in which the current is assumed to be parallel to the magnetic field so that there is no Lorentz force acting on the plasma. This can be written as

$$\nabla \times \mathbf{B} = \alpha \mathbf{B}, \quad (1)$$

where α is, in general, a function of space but is constant along every magnetic field line ($\mathbf{B} \cdot \nabla \alpha = 0$). A linear force-free extrapolation is based on the assumption that α is *everywhere* constant. This considerably simplifies the problem since, given an appropriate set of boundary conditions, the linear force-free field can be computed in a straightforward manner (see, e.g., Gary 1989).

It has been observed that at the photosphere, there is a wide distribution of α , so that one does not generally expect the coronal magnetic field to have a constant value of α . However, the difficulty of solving in general for a nonlinear force-free field means that many investigations have used linear force-free extrapolations of the coronal magnetic field, until recently, when several techniques for performing extrapolations of nonlinear force-free fields were developed (e.g., Amari et al. 1999; Wheatland et al. 2000; Wheatland 2004; Wiegmann 2004; Valori et al. 2005). These methods have been applied to test cases in which the solution is either a known analytic function or is the result of an MHD simulation. The performance of the method was typically then judged qualitatively on the basis of the appearance of selected magnetic field lines.

We present here a more quantitative method for judging the performance of an extrapolation technique, analogous to a method for determining quasi-separatrix layers (QSLs). Our method emphasizes where the extrapolation has been able to recover the topology of the field. For two test cases in which the solution is known, we extrapolate the field using both a linear force-free method and a nonlinear force-free method, and we compare subjective evaluation of the performance of the method with quantitative scores.

We have not included a wide range of different extrapolation techniques here, so we make no claim as to which is the best. Instead, we present a quantitative way to assess the performance of any method using known solutions. Our quantitative score shows that subjective evaluations may be misleading: in one of our examples, initial inspection of the results of the extrapolation suggests that it has performed quite well, even though it scores quite low. Thus, we conclude that even if an extrapolated field visually appears reasonable, care must be taken in drawing quantitative conclusions about the properties of the field.

¹ Current address: Colorado Research Associates Division, NorthWest Research Associates, Inc., 3380 Mitchell Lane, Boulder, CO 80301.

2. THE COMPARISON METHOD

A QSL is a region in which there is a steep gradient in field-line linkage (Priest & Démoulin 1995; Démoulin et al. 1996; Titov et al. 2002) and is a likely location for the formation of current sheets and reconnection. For field lines contained within a closed surface, it can also be thought of in terms of the mapping of field lines from one part of the boundary to another. In a QSL, neighboring field lines originating on one part of the boundary terminate a large distance apart on a different part of the boundary. In the context of reconnection, the most natural way to determine this is by looking for places in which the gradient of the mapping from one part of the boundary to another (or its inverse) is large. One measure of the size of gradient is the norm of the displacement gradient tensor (Priest & Démoulin 1995).

Another approach to locating QSLs is simply to look for large distances between footpoints of field lines originated from neighboring pixels (e.g., Metcalf et al. 2003). It is this approach that we adapt to quantify the performance of extrapolations where the true field-line mapping is known. Instead of looking for large differences between neighboring field lines, we compute the distance from the endpoint of the true field line to the endpoint of the extrapolated field line initiated at the same point on the boundary. If the extrapolation exactly matches the true field, then the distance between the endpoints will be zero; if the extrapolated field line diverges from the true field line, then the endpoints will likely lie far apart.

To be more precise about this, suppose that we are interested in field lines in a volume bounded by a closed surface S . Denote the parts of the surface through which field lines enter and leave the volume by S_0 and S_1 , respectively. In terms of a coordinate system (u, v) on the surface, the field line mapping $M : S_0 \rightarrow S_1$ takes a point $(u_0, v_0) \in S_0$ to a point $(u_1, v_1) = M(u_0, v_0) \in S_1$. Similarly, assuming the extrapolation preserves the normal component of the field on the boundary, the extrapolated field-line mapping takes the same point (u_0, v_0) to point $(u_1^e, v_1^e) = M^e(u_0, v_0)$. We score the performance of the extrapolation at each point on the boundary using the value of $d(u_0, v_0) = |(u_1, v_1) - (u_1^e, v_1^e)|$. If the extrapolation exactly reproduces the field, then $d = 0$. We choose to normalize d by the distance between the endpoints of the true field line, l . We refer to the normalized value of d as the field-line divergence (FLD).

To assign a single score to an extrapolation, we determine the fraction of the boundary that has field lines for which $d/l < p$, where we typically take $p = 0.1$. That is, we determine what fraction of the area of the boundary has field lines with less than a 10% FLD. In some cases, it may be more meaningful to normalize this to the flux and instead consider what fraction of the flux has field lines for which $d/l < p$, so for the examples presented here, we also quote this fraction.

The definition of the FLD has some of the same limitations as does using the distance for determining QSLs. For example, if the field lines are nearly tangent to the boundary when they intersect it, the distance between endpoints may be quite large even for field lines that track each other closely. Further, it is possible for a field line for the true solution and an extrapolated field line to have exactly the same endpoints, yet follow quite different paths to reach their endpoints. Such drawbacks could be addressed by, for example, considering the distance between the field lines averaged over the entire length of the field line.

Note that the FLD vanishes even on a QSL if the extrapolation exactly reproduces it but will have a very large value between the actual and extrapolated QSLs if they are not coincident. In this situation, a very small difference in the extrapolated and actual

magnetic field vectors at a point can produce a large difference in the field-line mapping. In effect, the FLD requires higher accuracy from the extrapolation in regions where neighboring field lines are diverging. However, if the extrapolated and actual QSLs are *only slightly* displaced, the overall score from the FLD can still be high, as the area (flux) of high FLD between the actual and extrapolated QSLs will be small. When considering processes that change the connectivity of the field (i.e., reconnection), it is crucial to get the field-line mapping correct. Further, QSLs are likely to be the locations of observational signatures of the field structure because energy released by reconnection can heat the plasma in this area. Comparison of extrapolations with, for example, the observed loop structure of the field will thus be highly sensitive to the location of QSLs. Therefore, we believe that higher accuracy in topologically important areas is an appropriate requirement for judging the performance of an extrapolation.

To highlight how the performance of an extrapolation method may appear good even though the topology of the field has not been successfully recovered, we also consider two of the measures of performance considered by Schrijver et al. (2006). The measures all give a quantitative evaluation of the performance of an extrapolation, but none of them focuses on the topology of the solutions. For comparison, we include here two of the measures, the Cauchy-Schwarz measure, defined as

$$C_{CS} = \frac{1}{M} \sum_i \frac{\mathbf{B}_i \cdot \mathbf{b}_i}{|\mathbf{B}_i| |\mathbf{b}_i|}, \quad (2)$$

and the mean vector error, defined as

$$E_n = \sum_i |\mathbf{b}_i - \mathbf{B}_i| / \sum_i |\mathbf{B}_i|, \quad (3)$$

where \mathbf{B}_i is the actual solution at grid point i , \mathbf{b}_i is the extrapolated field, and M is the total number of grid points. The first measure has a value of 1 if the field is reproduced perfectly, and subsequently we quote values of $1 - E_n$, which also has a value of 1 for a perfect extrapolation.

3. THE EXTRAPOLATION METHODS

To demonstrate our method for quantifying the performance of an extrapolation, we used two extrapolation techniques. The first technique was a standard implementation of the fast Fourier transform (FFT) method of calculating the linear force-free field for a given value of α (Gary 1989), while the second uses the nonlinear technique of Wheatland (2004). For the linear force-free extrapolation, we choose a value for α based on the approach described by Leka & Skumanich (1999), in which a single value of α is determined by minimizing the difference between the horizontal components of the actual and extrapolated fields on the boundary. Although our test cases certainly do not have constant α , the use of linear force-free extrapolations is so widespread that we use such an approach as a familiar standard that we expect to fail to some degree.

In order to mitigate the effects of the periodic boundary condition necessary for the Fourier transform, we surround the “photospheric magnetogram” with a region in which the normal component of the field vanishes. This is a compromise because to exactly match the normal component of the field on the boundary, the Fourier transform method must have oscillatory solutions in the vertical direction when $|\alpha| > 2\pi/l$, where l is the (largest) horizontal dimension of the region under consideration.

By increasing the dimensions of the region, we are reducing the maximum α that produces nonoscillatory solutions, in exchange for reducing the effect of the periodic boundary condition. In the first test case, we have $|\alpha| < 2\pi/l$, so no oscillatory solutions are present; in the second case, we have $|\alpha| > 2\pi/l$, so we can see the results of the oscillatory solutions.

Our second technique is that of Wheatland (2004), which is a current-field iteration approach to calculating nonlinear force-free fields. A number of lower boundary points are chosen as the footpoints for current-carrying field lines, and values of α are specified at these footpoints. A potential field \mathbf{B}_0 is calculated to match the normal component of the field at the lower boundary, and the field lines starting at the nominated footpoints are traced. Current is assumed to be distributed along these field lines to match the boundary values of α , provided the field lines do not leave the computational domain. Current is also assumed to be distributed along mirror field lines beneath the lower boundary, to preserve the boundary conditions on the normal component on the field. The field $\Delta\mathbf{B}_1$ due to these currents is calculated using an integral solution to Ampere's law, leading to a new field $\mathbf{B}_1 = \mathbf{B}_0 + \Delta\mathbf{B}_1$. The procedure is then repeated: the field lines of \mathbf{B}_1 starting at the nominated foot points are traced, and current is assumed to be distributed along these field lines, and so on. The procedure is halted when the field is changing sufficiently slowly at successive iterations.

The size of the grid on which the nonlinear extrapolation can construct the field is limited by the rate at which the CPU time scales with the dimensions of the grid, namely, fN^6 , where f is the fraction of boundary points with nonzero α and N is the linear dimension of the grid. Use of the FFT means that much larger grids are possible for the linear extrapolation. Thus, for both of our test cases, the linear extrapolation uses a grid spacing of $0.00625L$, while the nonlinear extrapolation uses a grid spacing of $0.01875L$. This difference is evident in a number of the figures as a reduction in the resolution of the norm of the displacement gradient tensor and of the field-line divergence.

Once we have extrapolated the field, we trace field lines in a volume limited in the horizontal directions to the area in which the boundary condition was input to the extrapolation, even when we have both the actual and extrapolated solutions for a larger volume. This results in some field lines that would otherwise have returned to the lower boundary intersecting the vertical sides of the box but does not result in a large loss of information, because the distance between endpoints for actual and extrapolated field lines can be calculated whenever both field lines end on the same face of the box, irrespective of which face that is. If the field lines end on different faces, then d is not defined; in this case, the field lines are typically diverging anyway.

4. THE TEST CASES

Solar energetic events are generally believed to draw on the energy available in the magnetic field, but the mechanism(s) by which this occurs is still under debate, with several competing models. In some models, the release of energy is driven by reconnection, either in a QSL (Mandrini et al. 1996; Schmieder et al. 1997; Démoulin et al. 1997a, 1997b; Bagalá et al. 2000), or by way of the separatrices associated with a coronal null point (Antiochos 1998, 1999); in another model, the release of energy is triggered by the kink instability (Fan & Gibson 2003, 2004; Török & Kliem 2003; Török et al. 2004). In our first test case, we consider a configuration with an X-type separator; in our second test case, we consider a twisted flux rope that is close to the stability limit. In each of these cases, there is a QSL that separates volumes of distinct magnetic connectivity. Thus, we have two

subjective assessments of the extrapolation: a visual comparison of field lines throughout the volume and a comparison of the location of QSLs, as determined by field lines in the QSL. The results of the subjective assessments will be compared to the quantitative score from the field-line divergence.

4.1. Case 1: An X-Type Separator

For our first case, we take the final step in a sequence of nonlinear force-free equilibria described by Chou & Low (1994). Specifically, in the notation of Chou & Low (1994), we take $\gamma = 5.4$, $r_0 = 1.3L/3$, and $a = L/2$, which is essentially the solution shown in their Figure 7c. The solution is azimuthally symmetric, with the axis of symmetry lying below the boundary for the extrapolations. The field is produced by a pair of monopoles on the axis below the boundary, just outside of a current-loaded sphere, plus their images in the sphere, and a term to remove the line singularity outside the sphere. For the parameters chosen, the boundary manifestation of this solution is a pair of strong, nearly potential “sunspots” bracketing a highly nonpotential pair of weaker “spots” (see Fig. 1, *left*). This configuration contains an X-type separator that intersects the boundary at $(x, y) \approx (0.0L, \pm 0.2L)$, which is a likely site for reconnection. For this example, the field is given in a region of the boundary $-0.75L < x < 0.75L$, $-0.75L < y < 0.75L$.

The right panel of Figure 1 shows field lines in the QSL, as determined by the norm of the displacement gradient tensor on the boundary (Priest & Démoulin 1995); the red line is a contour at a norm value of 10. One part of the QSL corresponds to the surface of the current-loaded sphere; it partitions the volume into field lines along which no current flows and twisted field lines along which a current does flow. The nature of the solution is such that the current is finite throughout the volume, but the current *density* becomes infinite as the surface of the sphere is approached from the inside (Chou & Low 1994). It is the discontinuous change to zero current density outside the sphere that causes the large displacement gradients across the surface.

Of more interest is the portion of the QSL that curls inward from the edge of the sphere toward the center of the weaker spots. This portion of the QSL is effectively separating field lines initiated in one of the weaker spots that terminate in the opposite polarity weaker spot from those that terminate in the inner portion of the stronger spot. The X-type separator is located within this portion of the QSL.

Finally, there are layers where neighboring field lines end on different faces of the box whose intersection with the lower boundary is shown in blue in the figure. In this case, the displacement gradient tensor is not well defined, because the surface of the box is not smooth (that is, the box has edges). The blue lines divide the lower boundary into six regions (not all simply connected) where field lines end on the six different faces of the box. For example, the small regions at $(x, y) \approx (\pm 0.65L, 0.0L)$ are where field lines end at $z = 1.25L$, while the triangular shape with vertices at $(x, y) \approx (-0.7L, \pm 0.5L)$, $(-0.55L, 0.0L)$ encloses field lines that end at $x = -0.75L$.

Figure 2 shows two qualitative evaluations of the linear force-free extrapolation with $\alpha = 1.7L^{-1}$. The left panel shows field lines for the true solution and the extrapolation, while the right panel shows the QSLs for the extrapolated field in the same manner as the QSLs for the analytic solution are shown in Figure 1. In some areas, the match between the two is clearly poor, while in other areas, it appears quite reasonable. For example, extrapolated field lines (*green lines*) in the top left corner of the plot rapidly diverge from the actual field lines (*red lines*), while along the central part of the neutral line there appears to be quite

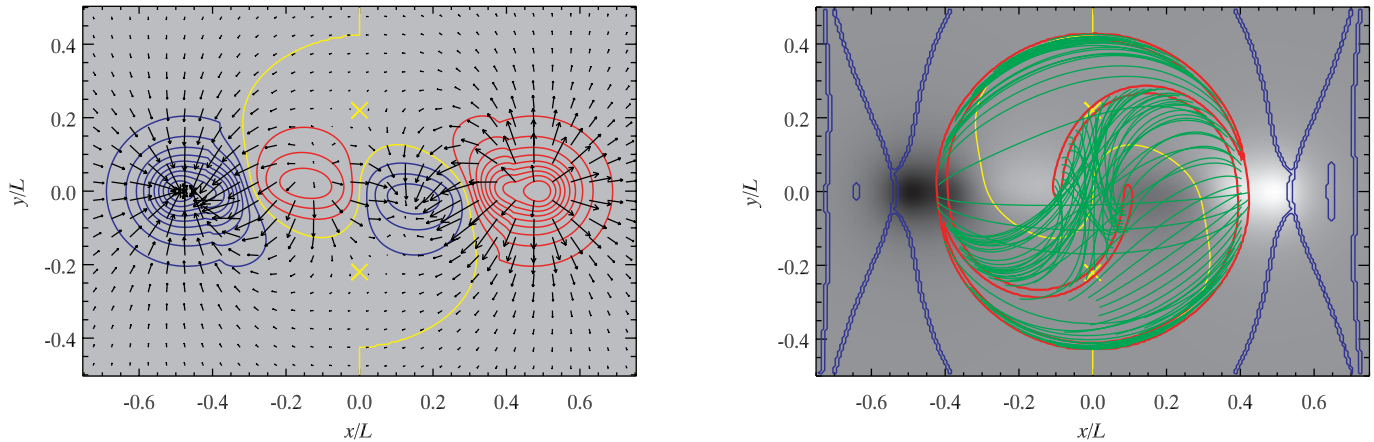


FIG. 1.—*Left*: Magnetic field on the boundary for the Chou & Low (1994) solution. Red and blue contours show the normal component of the field, while the neutral line is yellow. Arrows indicate the magnitude and direction of the horizontal field. An X-type separator (*yellow cross*) intersects the boundary at $(x, y) \approx (0.0L, \pm 0.2L)$ and is a likely site for reconnection. *Right*: Field lines (*green lines*) in the QSL, as determined by the norm of the displacement gradient tensor on the boundary; the red line is a contour at a norm value of 10. Gray scale shows the normal component of the field, with the neutral line in yellow. Blue lines indicate where neighboring field lines terminate on different faces of the box, i.e., where the displacement gradient tensor is not well defined.

good agreement. The location of the QSL provides support for this: in the interior of the current-loaded sphere, the location of the extrapolated QSL is similar to the actual QSL, but where the actual solution also has a QSL at the surface of the current-loaded sphere, the extrapolation contains no matching QSL. Despite the padding with zeros around the field of view, many of the extrapolated field lines still leave the edges of the box, as indicated by the blue contours that surround regions in which field lines terminate on the faces of the box at $y = \pm 0.75L$. In particular, the field lines in the bottom right and top left connect to images of the field of view produced by the periodic boundary conditions. Thus, we expect that the field within the current carrying sphere is generally reproduced quite well but that there are large differences in the extrapolation outside of the current carrying sphere.

However, visual inspection of the field lines does not provide a quantitative measure of the performance of the extrapolation. Thus, we turn to the FLD method described above for quantifying the performance of the extrapolated solution. Figure 3

shows the normalized distance between the ending footpoints of the true field lines and the extrapolated field lines in shades of blue, plotted at the location of the originating footpoint. The differences within the current-loaded sphere are generally less than 10% (*red contour*), although the location of the QSL is not exactly reproduced, leading to narrow bands of large difference in the mapping between the true location and the extrapolated location. Outside the current-loaded sphere, the agreement is not good at any point, with the large bands of gray where field lines connect to images of the field of view produced by the periodic boundary conditions.

The linear force-free extrapolation produces field lines with no more than a 10% error in only 27% of the area of the field of view and 67% in the current-loaded sphere. This is slightly misleading, as a significant fraction of the area that is poorly reproduced contains weak field, so the field lines with no more than a 10% error comprise 32% of the flux (74% in the sphere). Further, from the point of view of reconnection, the FLD shows that the interesting topology is fairly well reproduced, at the expense of

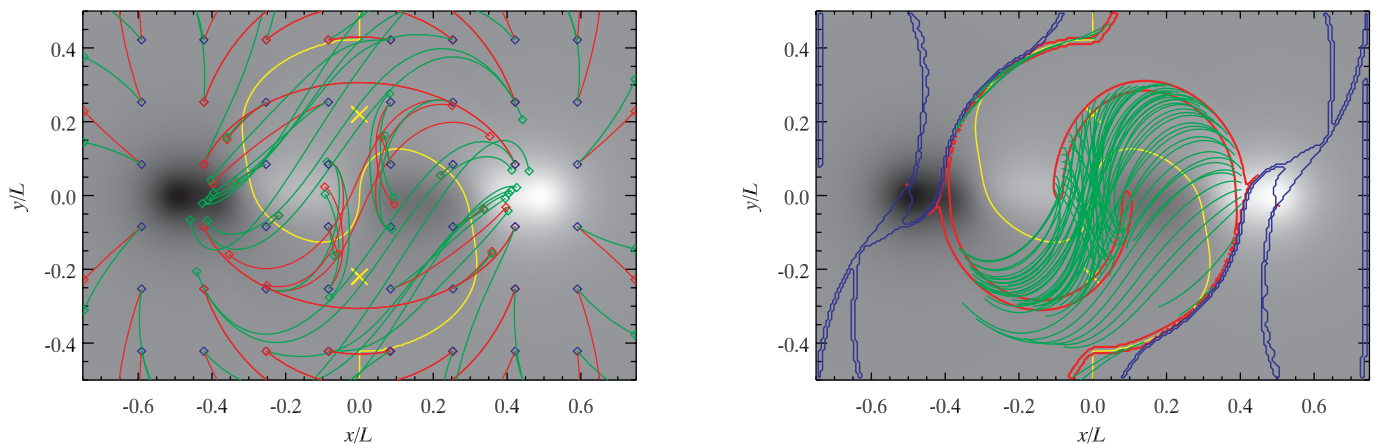


FIG. 2.—*Left*: Sample field lines for the Chou & Low (1994) solution (*red lines*) and for a linear force-free extrapolation of the field (*green lines*). Gray scale shows the normal component of the field, with the neutral line in yellow. There are evidently some areas where the two sets of field lines do not agree, such as field lines originating in the top left corner, where there is rapid divergence of the red and green lines. On the other hand, the short field lines across the neutral line near the center of the figure appear to agree quite well. *Right*: Similar to right panel of Fig. 1, but for the linear force-free extrapolation. For clarity, field lines are only initiated in positive-polarity regions where the displacement gradient tensor is large. The extrapolation does a reasonably good job of reproducing the QSL in the vicinity of the X-type separator but completely fails to reproduce the QSL at the boundary of the current carrying sphere.

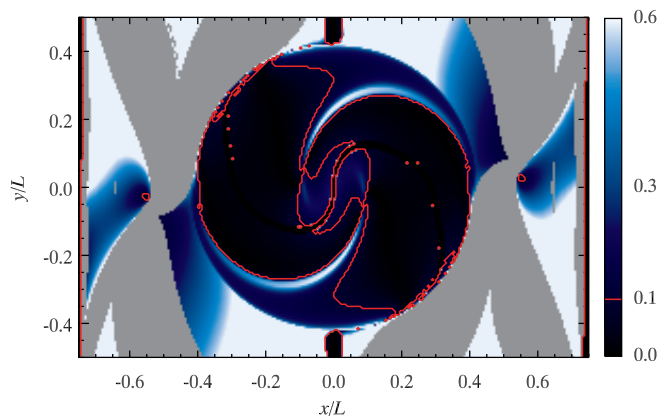


FIG. 3.—FLD for the linear force-free extrapolation of the Chou & Low (1994) solution, as measured by the normalized distance between endpoints of true and extrapolated field lines. Black regions have no difference between endpoints, while white has a large distance, as indicated by the color bar on the right; gray regions show field lines that end on different faces of the box. The red contour outlines the region in which there is less than a 10% difference in the normalized distance, which defines the quantitative score. The extrapolation does a good job of reproducing the solution within much of the current carrying sphere but is unable to reproduce the surrounding potential field and the exact location of the X-type separator.

the surrounding potential field. The other quantitative measures give fairly similar results: $C_{CS} = 0.82$ and $1 - E_n = 0.55$ for the whole volume, and $C_{CS} = 0.96$ and $1 - E_n = 0.86$ for the current-loaded sphere. The first two values indicate the extrapolation has performed neither particularly well nor particularly badly, while the second two show an improvement in the performance within the sphere.

Qualitative assessments of the nonlinear force-free extrapolation are shown in Figure 4. The nonlinear technique is generally able to reproduce the field lines that remain within the box very well, although there is some evidence that a few field lines do not exactly match, particularly those along the left and right sides, which leave the sides of the box. Turning to the QSLs, there are some small disagreements in comparison with Figure 1; in particular, the QSL around the outside edge of the sphere does not close on itself, as in the actual solution. Overall, however, the QSL appears to match quite well.

Using the FLD, shown in Figure 5, the nonlinear approach is correctly (less than 10% discrepancy) able to determine 55% of the field lines, carrying 68% of the flux within the entire field of

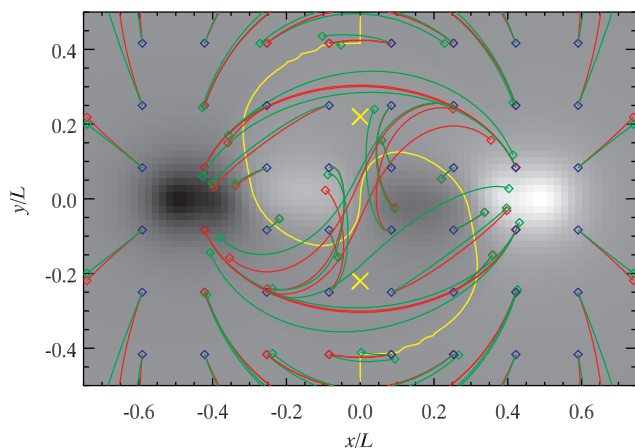


FIG. 4.—Similar to Fig. 2, but for the nonlinear force-free extrapolation. For field lines returning to the lower boundary of the box, the extrapolation generally does an excellent job of reproducing the solution.

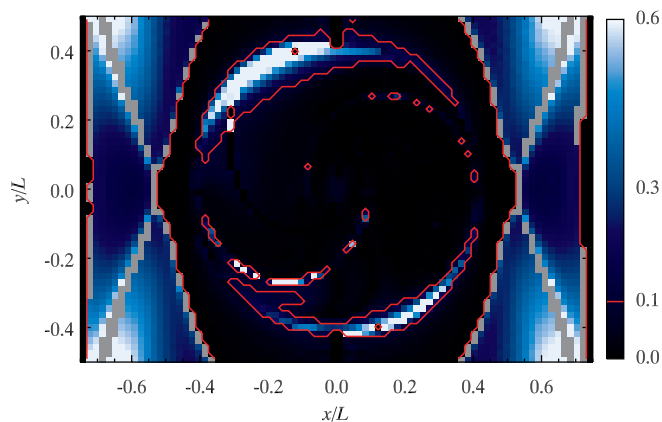


FIG. 5.—Similar to Fig. 3, but for the nonlinear force-free extrapolation. For field lines returning to the lower boundary of the box, the extrapolation generally does an excellent job of reproducing the solution, with the exception of small differences in the location of the edge of the current-loaded sphere. Note that $d = 0$ when a QSL is successfully reproduced, as in most of the inner part of the QSL shown here, but it is large between the extrapolated and actual QSLs when they are not coincident.

view, and 83% of the field lines and 94% of the flux within the current-loaded sphere. The main disagreement in the area (and flux) is caused by field lines that terminate on the sides and top of the box. The reason for this may be the symmetry of the problem: the Chou & Low (1994) solution has azimuthal symmetry about an axis below the boundary, while the extrapolation assumes the boundary is a plane of symmetry; thus, the currents outside of the volume in which the field is computed are quite different in the analytic solution compared to the extrapolation. There is also a minor difference in the location of the QSL surrounding the current-loaded sphere; this may well be a result of the discontinuity in the current across the edge of the sphere. The generally small values of the FLD in the interior of the sphere indicate that the QSL in which the X-type separator lies is reproduced very well, much better than for the linear extrapolation.

The other quantitative measures begin to show differences in this example. The scores are $C_{CS} = 1.00$ and $1 - E_n = 0.94$ for the entire volume, and $C_{CS} = 1.00$ and $1 - E_n = 0.96$ for the current-loaded sphere, all of which would suggest excellent agreement between the extrapolated and actual fields. Within the current-loaded sphere, these are comparable to the FLD measure, but there is no indication in these measures that outside of

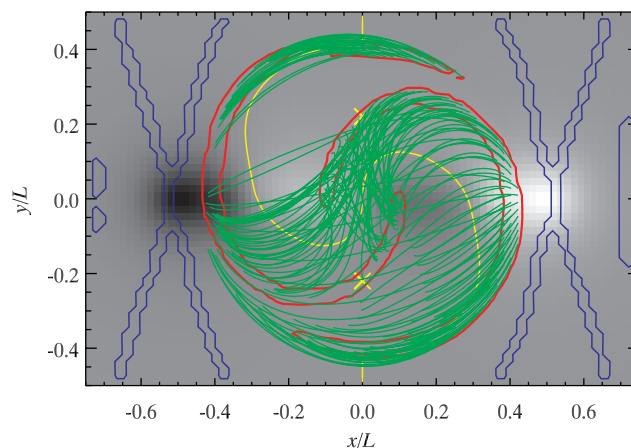


TABLE 1
SUBJECTIVE AND QUANTITATIVE SCORES FOR THE CHOU & LOW (1994) CASE

METHOD	OVERALL SCORE				SCORE FOR SPHERE			
	Subjective	C_{CS}	$1 - E_n$	FLD Area (Flux)	Subjective	C_{CS}	$1 - E_n$	FLD Area (Flux)
LFF.....	Fair	0.82	0.55	0.27 (0.32)	Good	0.96	0.86	0.67 (0.74)
NLFF.....	Good	1.00	0.94	0.55 (0.68)	Excellent	1.00	0.96	0.83 (0.94)

the sphere, there are systematic differences. Even though the angle between the direction of the extrapolated field and the direction of the actual field is small at essentially every grid point ($C_{CS} = 1.00$), if that angle is consistently in the same direction, it results in extrapolated field lines that diverge from the true field. Such is the case for field lines originating from $|x| \gtrsim 0.6L$, for example.

In both of these examples, subjective evaluation of the extrapolated field is confirmed by the FLD. In the case of the linear extrapolation, the results are fair for the whole field of view and improve somewhat if attention is confined to the current-loaded sphere. The nonlinear extrapolation has overall a good agreement with the actual solution and a generally excellent agreement for the current-loaded sphere. The other quantitative measures agree for the linear force-free extrapolation but begin to show differences for the nonlinear force-free extrapolation. These results are summarized in Table 1.

4.2. Case 2: A Bald Patch

For our second test case, we consider a simulation of the emergence of a twisted flux tube into an existing potential arcade performed by Fan & Gibson (2003, 2004). In this simulation, the emergence of the twisted flux tube is driven by applying an electric field at the lower boundary corresponding to lifting the flux tube into the corona. Before the flux tube becomes kink-unstable, the coronal field appears to evolve quasi-statically as the flux tube emerges, but to ensure that the system has come as close as possible to an equilibrium, we consider the final time step ($t = 64$) in a run in which the emergence of the flux tube was halted at time $t = 39$. At the time the run was halted, the axis of the flux tube had emerged, but it had not yet begun to kink. Thus, during the remainder of the run, the system is settling into a stable equilibrium.

Further, to ensure that the domain is force-free, we take as the boundary condition for the extrapolations the fifth grid point above the boundary of the simulation. The flux rope being emerged is not force-free, with the magnetic force at the boundary being balanced by gas pressure and viscosity terms. However, the solution becomes force-free just a few grid points above the simulation boundary (see Leka et al. 2005). We do not expect any force-free extrapolation to match the dynamical evolution of a kink-unstable flux tube or a field in which the magnetic force does not vanish, but we believe that this choice of boundary condition for the extrapolations should correspond to a force-free equilibrium.

Because the flux tube is twisted, and the axis of the flux tube has crossed the boundary (photosphere) at the time step we consider, there must be a bald patch along part of the neutral line separating the opposite-polarity footpoints of the flux tube (see Fig. 6). Roughly, a bald patch can be thought of as a section of neutral line along which the horizontal field points from negative polarity to positive polarity, indicating a dipped field. More rigorously, Titov et al. (1993) require that in a bald patch $B_z = 0$ and $\mathbf{B} \cdot \nabla B_z > 0$, where B_z is the normal component of the field. In the simulation, continued emergence of the flux tube results in the formation of a current sheet near the bald patch separatrix surface, indicating possible reconnection and heating. The separatrix surface appears as a QSL in the right panel of Figure 6. Gibson et al. (2004) argue that this current sheet can explain the shape and handedness of X-ray sigmoids. Thus, reproducing the bald patch separatrix surface is critical for an extrapolation to be useful.

In Figure 7 we show sample field lines and QSLs for a linear force-free extrapolation of the simulation, with $\alpha = -9.6L^{-1}$. There are clearly many areas where the field lines do not match well, for example in the bottom right and top left corners, where the field lines immediately start to diverge. There is a suggestion

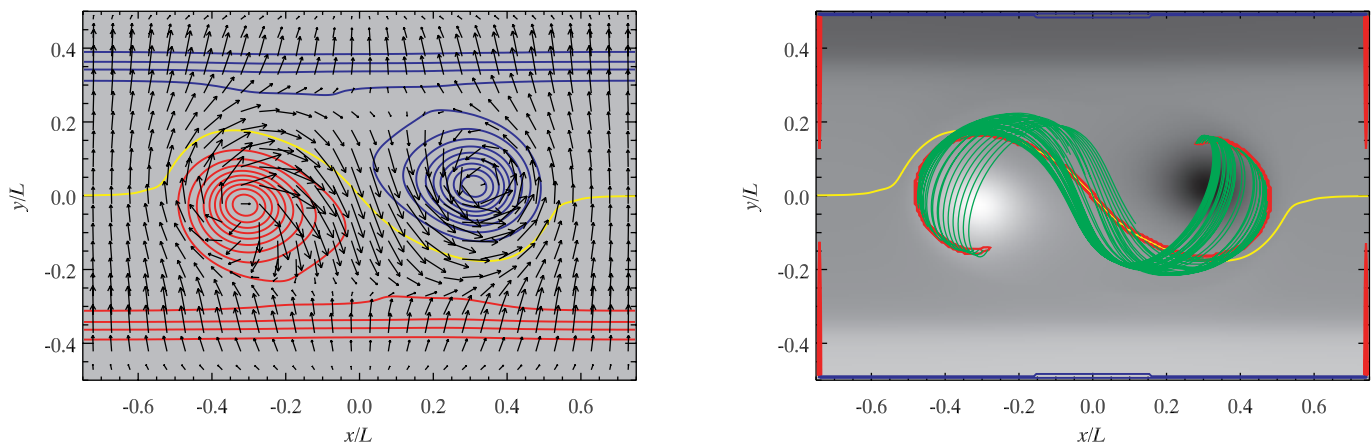


FIG. 6.—Similar to Fig. 1, but for the simulation of Fan & Gibson (2003, 2004). The footpoints of the flux tube are centered at $(x, y) \approx (\pm 0.35L, 0.0L)$, while the arcade is in the region $0.35L \lesssim |y| \leq 0.5L$. There is a bald patch on the neutral line between the footpoints of the flux tube; the associated separatrix surface appears as a QSL in the right panel.

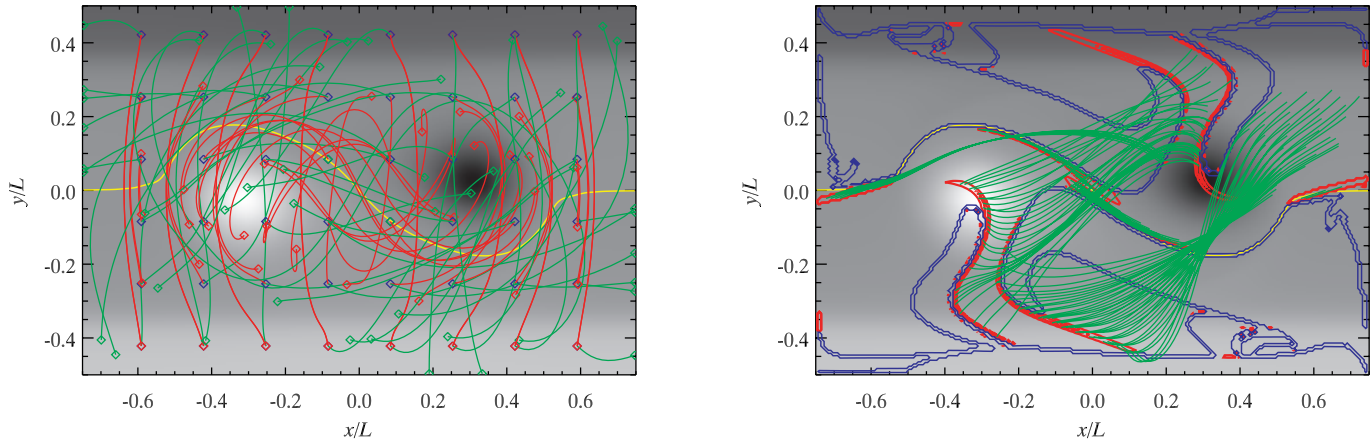


FIG. 7.—Similar to Fig. 2, but for the linear extrapolation of the simulation of Fan & Gibson (2003, 2004). There are clearly large differences between the extrapolated field lines and the field lines in the simulation. Although the extrapolation has QSLs associated with bald patches, their shape bears little resemblance to the simulation.

that in the center of the flux tube, both sets of field lines are S-shaped, but it immediately becomes apparent from the QSLs that the linear force-free extrapolation does not reproduce this case well. Although there are bald patches present, they include sections of the neutral line outside of the flux tube footpoints. The corresponding QSLs are nothing like the shape of the bald patch separatrix surface in the simulation, and there are several other QSLs that are completely absent in the simulation.

The FLD plot (Fig. 8) confirms this, indicating that the field lines match to within 10% on only 4% of the boundary, containing 7% of the flux, mainly near the center of the flux tube. The correspondence in this location is not surprising, since the value of α used is representative of the flux tube. However, the linear extrapolation is unable to reproduce even the majority of the flux tube, in part because of the oscillatory solutions required by the highly twisted nature of the flux tube. This is further confirmed by the extremely low values of the other quantitative measures: $C_{CS} = 0.04$ and $1 - E_n = -2.39$.

Finally, we turn to the nonlinear extrapolation of the flux tube, starting with the sample field lines and the QSLs shown in Figure 9. Initial inspection suggests that it may do better. There are clearly some highly twisted field lines within the flux tube and some potential field lines forming an arcade over the flux tube, although a few extrapolated field lines (e.g., those in the

top left corner) are clearly diverging from the field lines in the simulation. The extrapolation does result in a bald patch along the neutral line between the footpoints of the flux tube, with a corresponding separatrix surface that is inverse S-shaped. Qualitatively, this matches the MHD solution shown in Figure 6, although it can be seen that the location of extrapolated separatrix surface away from the bald patch does not exactly match. In fact, this qualitative agreement is misleading, when the results of the FLD are considered.

The FLD shown in Figure 10 indicates that the extrapolation has difficulty with both the flux tube and the surrounding arcade. It successfully (less than 10% difference) reproduces field lines from 28% of the boundary, accounting for only 18% of the flux. In contrast, the other quantitative measures suggest that the extrapolation is at least a fair representation ($1 - E_n = 0.53$), if not a good one ($C_{CS} = 0.92$), of the actual field.

The discrepancies in the arcade field lines are due, at least in part, to the perfectly conducting boundary conditions imposed in the numerical simulation, which prohibit field lines from intersecting the side walls of the box. In the extrapolation, no such confinement occurs, so the potential arcade expands to fill a much larger volume. This accounts for the large bands of gray around the edges of the lower boundary, where extrapolated field lines intersect the faces of the box, while true field lines cannot. In the Sun, the situation may lie somewhere between these two extremes. Other active regions will prevent the field from expanding completely; yet unless there is strong flux immediately outside the area being considered for the extrapolation, the confinement will be less extreme than in the simulation. This difference indicates the possible limitation of considering an active region in isolation of everything else present on solar disk.

In the flux rope, the failure of the extrapolation to exactly match the simulation may be a result of the amount of current present. In order for the extrapolation to converge, not all of the current crossing the boundary can be included. Thus, one certainly expects some differences between the extrapolated solution and the simulation. While the sample field lines and QSL clearly indicate that a flux rope is present in the extrapolation, it does not match in detail the flux rope present in the MHD solution. As in the previous case, there are areas of very large FLD where the extrapolated location of the QSL (in this case, the bald patch separatrix surface) does not match the actual location. Such is the case in the vicinity of $(x, y) \approx \pm(0.3, 0.3)$. Note that if a bald patch is present in the extrapolation, it cannot be

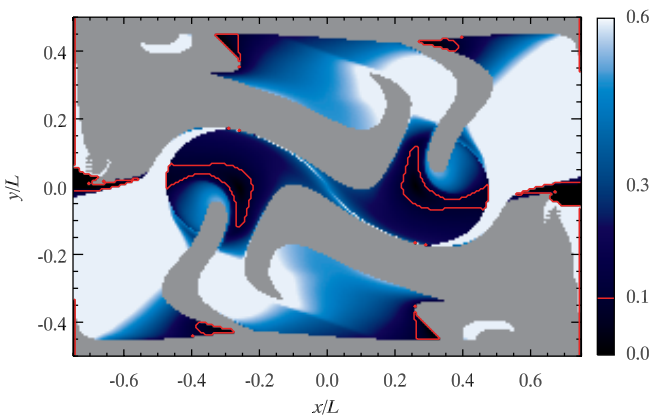


FIG. 8.—Similar to Fig. 3, but for the linear extrapolation of the simulation of Fan & Gibson (2003, 2004). There is a small area near the center of the flux tube in which the extrapolated field lines are close to the field lines from the simulation, but overall there is little resemblance.

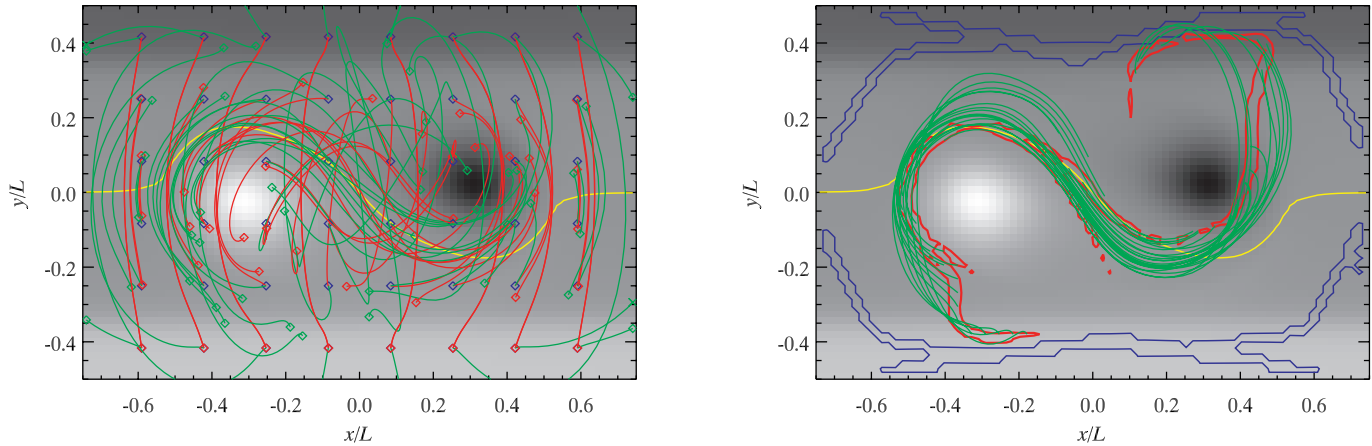


FIG. 9.—Similar to Fig. 2, but for the nonlinear extrapolation of the simulation of Fan & Gibson (2003, 2004). The extrapolated field lines do indicate the presence of a flux tube with an overlying arcade, although there are still clear differences in some places, such as in the top left corner. The extrapolation also has a QSL that is qualitatively similar to the bald patch separatrix surface in the simulation.

displaced with respect to the true bald patch because that would change the location of the neutral line, which is impossible for an extrapolation that exactly reproduces the normal field on the boundary. However, the extent of the bald patch along the neutral line does not have to be exactly reproduced, as that depends on the horizontal components of the extrapolated field, which may not be exactly reproduced.

Near the axis of the flux rope, the FLD is also large, typically 30%–40%. If an extrapolated field-line winds about the axis of the flux rope a different number of times than the actual field line, it will have a nonzero FLD (unless the difference is an integer number of winds and the axis is accurately reproduced). Thus, the significantly nonzero values of the FLD within the flux rope indicate that the extrapolated field does not contain the same number of winds as the simulation field. The extrapolation may be useful for qualitative conclusions, such as inferring the *existence* of the flux rope, but any quantitative results, such as determining the helicity present and hence whether the flux rope is likely to be kink-unstable, cannot be obtained from the extrapolation.

In comparison to our first test case, neither subjective examination of these examples nor other quantitative measures completely agrees with the results of the FLD scores, as summarized in Table 2. In the case of the linear force-free extrapolation, it is

easy to conclude by any means of judging that the extrapolation has performed poorly. However, for the nonlinear extrapolation, inspection of the resulting field-line appearance and other quantitative measures suggest a reasonable agreement that is not confirmed by the FLD score.

5. DISCUSSION

Can force-free extrapolations successfully reproduce the magnetic field in the Sun’s corona? To answer this, it is necessary to have a quantitative measure of success when the true field is known. We have presented here one such measure, based on the divergence of an extrapolated field line from the true field line originated at the same point on the boundary.

For cases in which the extrapolation performs either extremely well or extremely poorly, it is comparatively straightforward to judge the performance of the extrapolation. For the nonlinear extrapolation of our first example, the analytic solution of Chou & Low (1994), sample extrapolated field lines closely match the locations of the true field lines, and the QSLs are in approximately the same locations. This is borne out by the high field-line divergence (FLD) score, particularly within the current-loaded sphere. Similarly, for the linear extrapolation of our second example, the MHD simulation of Fan & Gibson (2003, 2004), the sample extrapolated field lines bear no resemblance to the true field lines, and there is little correspondence between the locations of the QSLs. Once again, this is confirmed by the extremely low FLD score.

However, in intermediate cases, qualitative visual comparison of the extrapolation to the real solution can be misleading. For the linear extrapolation of the first example, there are clearly extrapolated field lines that are wildly different from the true field lines, but the FLD shows exactly where there is reasonable agreement and indicates that, although the extrapolation fails to reproduce the

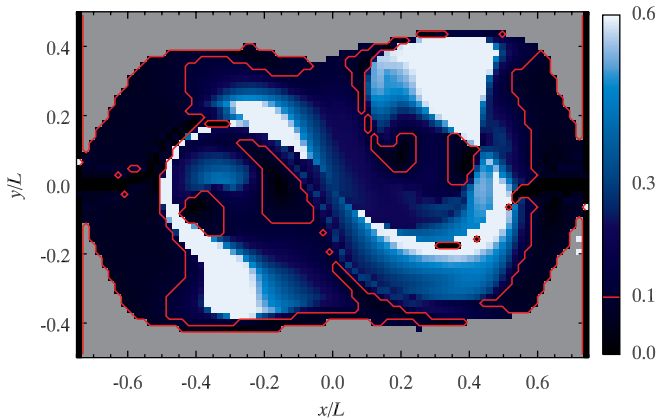


FIG. 10.—Similar to Fig. 3, but for the nonlinear extrapolation of the simulation of Fan & Gibson (2003, 2004). The extrapolation is able to successfully reproduce only a part of the arcade and a small volume in the center of the flux tube, indicating that despite the qualitative similarity to the true solution, it has not accurately reproduced much of the field.

TABLE 2
SUBJECTIVE AND QUANTITATIVE SCORES FOR THE FAN & GIBSON (2003, 2004) CASE

METHOD	SCORE			
	Subjective	C_{CS}	$1 - E_n$	FLD Area (Flux)
LFF.....	Poor	0.04	-2.39	0.04 (0.07)
NLFF.....	Good	0.92	0.53	0.28 (0.18)

surrounding field, the topologically interesting X-type separator is in fact quite well reproduced. More importantly, for the nonlinear extrapolation of the flux tube, there are extrapolated field lines that clearly twist in the right sense within the flux tube, plus an overlying potential arcade. Even the QSL is qualitatively the correct shape. However, the FLD score indicates that the subjective evaluations are not correct: the extrapolation has failed to reproduce the correct twist of the flux tube, so any quantitative measure of, for example, the helicity present will not be correct.

We have demonstrated here the limitation of even a nonlinear force-free extrapolation technique for reproducing a highly twisted flux tube. Does this mean that extrapolations are not a useful tool? No. We simply conclude that no quantitative analysis should be done using this particular extrapolation technique for configurations containing large amounts of current. More importantly, we have established a method by which other techniques can be judged, to see if any are appropriate for reconstructing such highly nonpotential configurations. Subjective comparisons of field lines,

and even comparisons of QSLs, can be misleading in judging the performance of an extrapolation. Thus, we propose the FLD method as a way of assessing the performance of extrapolations when the true solution is known.

The National Center for Atmospheric Research is sponsored by the National Science Foundation. Funding is gratefully acknowledged from the Air Force Office of Scientific Research under contract F49620-02-C-0191 and from the National Science Foundation under grant ATM 04-54610. M. S. W. acknowledges the support of an Australian Research Council QEII Fellowship. We thank Sarah Gibson and Cristina Mandrini for helpful discussion, Yuhong Fan for providing the MHD simulation data and valuable comments on the manuscript, and Tom Metcalf for the use of his implementation of the linear force-free extrapolation method. We also thank the referee for helpful comments that strengthened our results.

REFERENCES

- Amari, T., Boulmezaoud, T. Z., & Mikic, Z. 1999, *A&A*, 350, 1051
 Antiochos, S. K. 1998, *ApJ*, 502, L181
 Antiochos, S. K., DeVore, C. R., & Klimchuk, J. A. 1999, *ApJ*, 510, 485
 Bagalá, L. G., Mandrini, C. H., Rovira, M. G., & Démoulin, P. 2000, *A&A*, 363, 779
 Brosius, J. W., Landi, E., Cook, J. W., Newmark, J. S., Gopalswamy, N., & Lara, A. 2002, *ApJ*, 574, 453
 Chou, Y. P., & Low, B. C. 1994, *Sol. Phys.*, 153, 255
 Démoulin, P., Bagalá, L. G., Mandrini, C. H., Hénoux, J. C., & Rovira, M. G. 1997a, *A&A*, 325, 305
 Démoulin, P., Hénoux, J. C., Mandrini, C. H., & Priest, E. R. 1997b, *Sol. Phys.*, 174, 73
 Démoulin, P., Hénoux, J. C., Priest, E. R., & Mandrini, C. H. 1996, *A&A*, 308, 643
 Fan, Y., & Gibson, S. E. 2003, *ApJ*, 589, L105
 ———. 2004, *ApJ*, 609, 1123
 Gary, G. A. 1989, *ApJS*, 69, 323
 Gibson, S. E., Fan, Y., Mandrini, C., Fisher, G., & Démoulin, P. 2004, *ApJ*, 617, 600
 Leka, K. D., Fan, Y., & Barnes, G. 2005, *ApJ*, 626, 1091
 Leka, K. D., & Skumanich, A. 1999, *Sol. Phys.*, 188, 3
 Lin, H., Kuhn, J. R., & Coulter, R. 2004, *ApJ*, 613, L177
 Mandrini, C. H., Démoulin, P., van Driel-Gesztelyi, L., Schmieder, B., Cauzzi, G., & Hofmann, A. 1996, *Sol. Phys.*, 168, 115
 Metcalf, T. R., Alexander, D., Hudson, H. S., & Longcope, D. W. 2003, *ApJ*, 595, 483
 Priest, E. R., & Démoulin, P. 1995, *J. Geophys. Res.*, 100, 23443
 Schmieder, B., Aulanier, G., Démoulin, P., van Driel-Gesztelyi, L., Roudier, T., Nitta, N., & Cauzzi, G. 1997, *A&A*, 325, 1213
 Schrijver, C. J., et al. 2006, *Sol. Phys.*, in press
 Titov, V. S., Hornig, G., & Démoulin, P. 2002, *J. Geophys. Res.*, 107, 3
 Titov, V. S., Priest, E. R., & Démoulin, P. 1993, *A&A*, 276, 564
 Török, T., & Kliem, B. 2003, *A&A*, 406, 1043
 Török, T., Kliem, B., & Titov, V. S. 2004, *A&A*, 413, L27
 Valori, G., Kliem, B., & Keppens, R. 2005, *A&A*, 433, 335
 Wheatland, M. S. 2004, *Sol. Phys.*, 222, 247
 Wheatland, M. S., Sturrock, P. A., & Roumeliotis, G. 2000, *ApJ*, 540, 1150
 Wiegmann, T. 2004, *Sol. Phys.*, 219, 87